Microwave Photonics—Design of a Fiber Optic Recirculating Loop

Diamond M. Moody and James A. Shackford

ABSTRACT

This article outlines recent Johns Hopkins University Applied Physics Laboratory (APL) work on a fiber optic recirculating loop (RCL) system and describes some of the important design decisions. Optical RCLs were originally designed as a means to study long-haul data transmission systems in a compact, less-expensive manner. For this project, however, the RCL is used to transmit repeated radio frequency (RF) signals within a larger optical system. At its core, an RCL consists of a length of fiber and an amplifier. An optical switch is used to let an encoded RF signal enter the loop, while an optical coupler is used to let the encoded RF signal exit the loop. We made multiple design decisions while making this system. Most important, chromatic dispersion of the optical fiber disrupts transmission of the recirculated RF signal. To account for this, we evaluated multiple optical fiber types, encoded the RF signal using a single-sideband technique, and incorporated a programmable optical filter with dispersion compensation capabilities. Moreover, polarization-dependent loss (PDL) and polarization-mode dispersion (PMD) within optical components are compounded as light recirculates. To accommodate for this, we incorporated a polarization scrambler in the design. In this article, we walk through the RCL design process and mention the contributions of each optical component to the final design.

INTRODUCTION

Photonics is the science of the generation, control, and detection of light. The photon is the elementary particle of light. Photonics involves the flow of photons like electronics involves the flow of electrons. Microwave photonics involves devices that operate in microwave frequencies, which range from 1 GHz to 1 THz (30- to 0.03-cm wavelengths). Since the field encompasses optical, microwave, and electrical engineering, microwave photonics spans frequencies below 1 kHz (radio frequency, or RF) to hundreds of terahertz (optical). Microwave photonic technology has been implemented in scientific, military, and commercial applications. It plays an important role in high-bit-rate data transmission, the remoting of antennas for satellite and cellular radio applications, cable television signal distribution, optoelectronic probing of devices and circuits, and optical signal processing.[1]

Microwave photonics has several advantages over traditional electronics. These include broader bandwidth, reduced electromagnetic interference, more tunability, reconfigurability, and reduced SWaP (size, weight, and power). Furthermore, fiber optic cables have low loss (compared with coaxial cables). The aforementioned advantages in photonics allow for signal processing using analog photonic link delay lines rather than coaxial cable delay lines or the digital signal processing that modern RF systems often use. A photonic link first converts an RF signal into an optical signal. Then, the processing is performed in the optical domain. Finally, the optical signal is converted back into the RF domain.

Members of APL's Optics and Photonics Group developed a prototype photonic system with multiple delay line options. This article describes the recirculating loop (RCL) delay line module. The technical objective of the RCL was to generate multiple repeated copies of a short-duration input RF signal. The project included building and testing a lab prototype for single-wavelength operation, further developing the prototype to function for multiple-wavelength operation, and assembling the final system. In this article, we describe the concept, design, and operation of this RCL system.

BACKGROUND

Recirculating Loop

A photonic RCL is a fiber optic system typically used for studying long-haul transmission systems in optical fiber communications. A typical long-haul transmission system consists of a transmitter, a long length of optical fiber, intermittently spaced amplifiers to counteract fiber losses, and a receiver (Figure 1a). It would be impractical to build such a system in a lab. The transmission portion of a long-haul system is seemingly periodic, with equally spaced amplifiers and
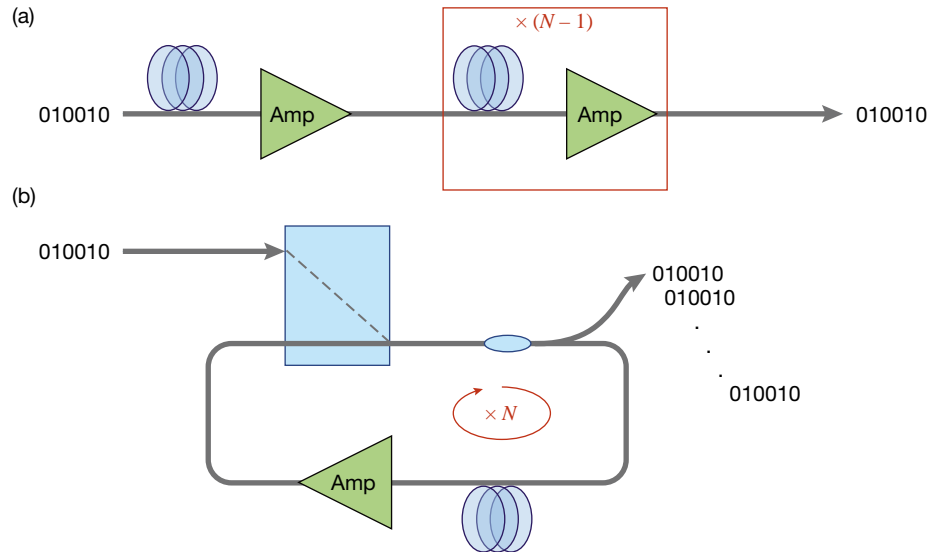
lengths of fiber. An RCL takes advantage of this periodicity—long-distance systems can be recreated using a moderately long fiber and a single amplifier, provided the light makes multiple round trips through this system. This simple RCL architecture is shown in Figure 1b. In reality, an RCL does not behave the same way as a long-haul system because of its true periodic nature.

Instead of studying long-haul data transmission systems, we use an RCL to transmit analog RF signals. The RCL generates multiple copies of an input RF signal that decay in quality over multiple circulations. To mitigate this decay, we use various techniques and design decisions, discussed in the section on design.

Encoder/Decoder

To generate repeated copies of the signal in the optical domain, we need to first convert the RF signal into an optical one with an encoder. Our encoder includes an electro-optic (E/O) modulator and a bandpass filter (Figure 2). An E/O modulator is a device that can
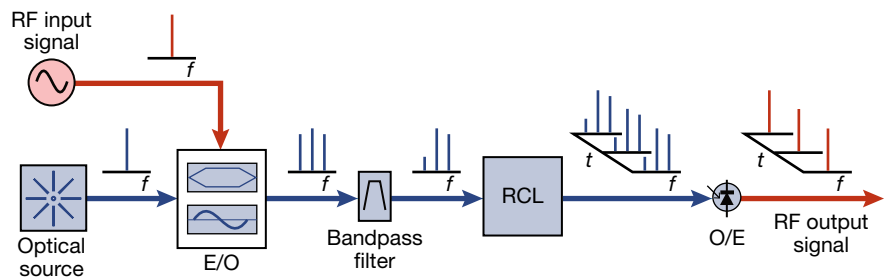

Figure 1. Typical long-haul transmission system (a) and basic RCL architecture (b). RCL architecture is more practical to build in a lab and, thus, is used to emulate long-haul transmission systems.

Figure 2. Block diagram of encoder, RCL, and decoder. The optical signal is modulated by an RF signal using either intensity or phase modulation. Then, a bandpass filter is used to convert the DSB signal into SSB. The RCL generates repeated copies of the signal in the optical domain. Finally, the optical signals are converted back into the RF domain using a photodiode.

modulate an RF signal onto an optical carrier so that operations can be performed in the optical domain. In our system, we have the option to use either intensity or phase modulation. Within the encoder, the signal is filtered down to single-sideband (SSB) using a filter. Using an SSB instead of a double-sideband (DSB) signal will reduce the effects of chromatic dispersion, which is detailed in the section on optical fiber. In the early development stages, we wanted to demonstrate working performance for a single wavelength that was chosen to optimize gain flatness. Later stages of the project focused on supporting operation for 16 wavelengths simultaneously. In this case, the 16 optical carriers are combined onto a single fiber using a technique known as wavelength division multiplexing (WDM).

Figure 3. Block diagram of RCL fiber optic delay line. The design consists of (1) a gate block, (2) a programmable optical filter, (3) polarization control, (4) a switched delay architecture, and (5) amplification.

After the signal exits the coupler, we need to convert the optical signals back into an RF one with a decoder. This is achieved by using a photodetector (Figure 2). Within the loop of the RCL, a fiber coupler is used to split the signal onto a photodetector. In a fiber coupler, the cores of fibers are in contact, allowing the light to be split and/or combined between the fibers. The amount of light that goes through each output is determined by the how much the fibers overlap. The amount of light going into the loop and onto the photodetector is an important consideration when choosing an optimal coupling ratio. If too much light is sent to the photodetector, the recirculating signal in the loop is indistinguishable from the noise, especially after multiple instances of recirculation. On the other hand, sufficient light must go to the photodetector to be detected at the output. Thus, we determined that it was appropriate to use a coupler with a 50/50 coupling ratio at the output.

DESIGN

Overview

Our RCL design consists of five main components, as shown in Figure 3: a gate block, a programmable optical filter, polarization control, a switched delay architecture, and an amplifier. Intensity- or phase-modulated light is first input to the gate block, which operates in two s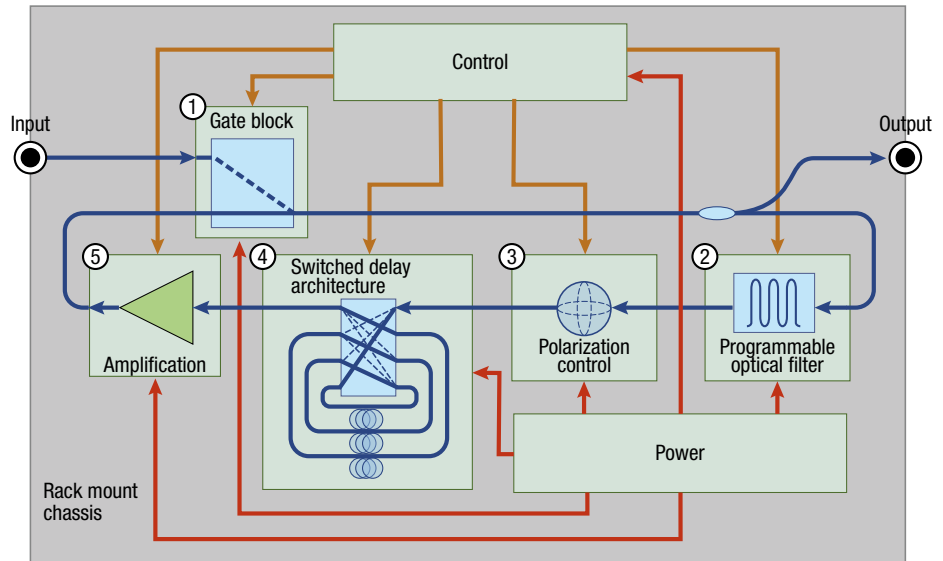tates—a load state and a recirculating state. After being loaded into the system, the light passes through the optical filter where excess noise is filtered out and some dispersion compensation is applied. The light then travels through a polarization scrambler, which helps compensate for polarization-mode dispersion (PMD). Afterward, a long length of fiber is selected via the switched delay architecture, and light travels a distance from 4 km up to 28 km. Finally, the light is amplified so it matches the power at which it was originally loaded. The light circulates through this loop multiple times, and with each circulation it is monitored via an output tap.

In the following sections, we discuss the design decisions for each subsystem in order of how critical it is to the overall system design. First, we discuss our optical fiber type options and selection. Then, we discuss the main components in the following order: switched delay architecture, gate block, amplification, programmable optical filter, and polarization control. Finally, will discuss the mechanical design, power, and control of the final system.

Optical Fiber

To generate repeated copies of the original with high fidelity, we have to consider the optical fiber type and its properties. Optical fibers can be either single-mode fiber (SMF) or multimode fiber (MMF). MMFs have a larger core diameter and can transmit multiple modes of light simultaneously. Therefore, MMFs are affected by modal dispersion, which is dispersion caused by the time delay between different modes at a given frequency.[4] This limits the acceptable length of fiber in fiber optic systems. Since we are using several kilometers of fiber,

MMF is not a good option for our application. Since SMFs only allow one mode to propagate, they do not suffer from modal dispersion.

Within SMFs, there is the option to use polarization-maintaining (PM) fibers. PM fibers have a linear bire-fringence that maintains the linear polarization of linearly polarized light properly launched into the fiber. While PM fibers would simplify the mitigation of polar-ization effects such as polarization-dependent gain/loss (PDG/PDL) and PMD, they are expensive. Since long lengths of fiber (e.g., 28 km) would be costly, we chose to use non-PM fibers in our design. To mitigate the polarization effects that occur in non-PM fibers, we use a polarization scrambler, discussed in the section on polarization control.

The final consideration is the dispersion that occurs in optical fiber. The RCL required RF responses up to 40 GHz across seven lengths of fiber, ranging from 4 km (20-μs delay) to 28 km (160-μs delay). Ideally, we want the RF response at the photodetector to be a constant function of frequency for any length of fiber. However, the index of refraction of an optical fiber is dependent on the frequency of the light that passes through it. Therefore, light at different frequencies travels at differ-ent speeds along the fiber optic cable. This phenomenon is known as chromatic dispersion. Chromatic dispersion in SMF is the sum of material and waveguide dispersion. For optical fiber, dispersion is expressed in picoseconds per nanometer per kilometer, which can be understood as picoseconds of delay between two colors of light sepa-rated by 1 nm in wavelength per kilometer of fiber. The linear RF transmission is proportional to

$$T \propto \sin^2 \left(\frac{\pi \lambda^2 f^2 D L}{c} \right) \qquad (1)$$

for an intensity-modulated signal and

$$T \propto \cos^2 \left(\frac{\pi \lambda^2 f^2 D L}{c} \right) \qquad (2)$$

for a phase-modulated signal, where λ is the optical car-rier wavelength, f is the RF frequency, D is the dispersion parameter, L is the fiber length, and c is the speed of light in vacuum.[5] Dispersion causes the RF response to change depending on the length of fiber over which the light travels and the RF frequency. The RF power varies strongly as a function of frequency and transport length and can be very weak when the cosine or sine terms approach zero. Note that the null responses for phase and intensity modulation are complementary. This behavior is undesirable because we want to reproduce the input signal with high fidelity for each circulation.

To mitigate the effects of chromatic dispersion, we considered different types of SMFs. Foremost, standard single-mode fiber (SSMF) is historically the most com-monly used optical fiber, and is the cheapest and most readily available.[6] We also considered dispersion-shifted

fiber (DSF), which eliminates dispersive fading at 1,550 nm but typically is not used because of unwanted nonlinear optic effects.[7,8] Finally, we considered non-zero-dispersion-shifted fiber (NZ-DSF), which has low but non-zero dispersion at 1,550 nm and is exten-sively deployed as an optical communications fiber.[9] NZ-DSFs typically come in two families, NZD+ and NZD−, which have a zero-dispersion wavelength lower and higher than 1,550 nm, respectively. The results for NZ-DSF+ and NZ-DSF− are equivalent since Eqs. 1 and 2 are independent of sign. The optical specifications for these fiber types are summarized in Table 1.

Table 1. Optical specifications for optical fibers[7,10,11]

Fiber Type	Zero-Dispersion Wavelength (nm)	Attenuation (dB/km) at 1,550 nm	Chromatic Dispersion at 1,550 nm (ps/nm/km)
SSMF	1,304–1,324	≤0.17	≤18
DSF	1,525–1,575	≤0.35	≤3.5
NZ-DSF+	~1,500	≤0.19	≤6.0

We narrowed our selection to the SSMF and NZ-DSF fiber types based on availability and costs. To select between the two fiber types, we modeled intensity and phase-modulated transport of RF signals using Eqs. 1 and 2 for both types (Figure 4). Plots a–d in Figure 4 show the RF transmission as a function of RF frequency and transport time, which is related to the fiber length.

The SSMF transmission (Figure 4, a and b) has a lot of variation, especially at longer transport times and higher RF frequencies. The intensity-modulated signal would only be able to go up to about 2 GHz without getting a strong null for the entire transport duration. The NZ-DSF transmission (Figure 4, c and d) has less variation than SSMF. The intensity-modulated signal could go up to about 6 GHz without getting a strong null for the entire transport duration. Although the behavior is better than SSMF, it is still not ideal for long distances and high fre-quencies. To further address the dispersion, we use an SSB signal from the encoder and apply additional dispersion compensation, as discussed in the sections on the pro-grammable optical filter and characterization. Plots e and f in Figure 4 show transmission of SSMF and NZ-DSF fiber types at 10 GHz as a function of time. Again, NZ-DSF fiber has significantly less variation than SSMF. For this reason, we chose NZ-DSF as our fiber type.

Switched Delay Architecture

For this RCL design, one requirement was a switch-able delay line length with seven distances from 4 km up to 28 km in 4-km increments. For the switched delay architecture, we selected a 4 × 4 microelectromechanical system (MEMS) matrix switch to perform this capability,

with the design shown in Figure 5. Using a matrix switch allows for simultaneous connections between the inputs and outputs of the switch. Any input can be routed to any output. By setting up the fiber lengths in a binary sequence of 4-km fiber spools as shown, we can increment the fiber length choice by 4 km. For example, as drawn the light would travel 28 km by going through the 4-km, then 8-km, then 16-km paths. Since light travels through all three fiber paths, this is equivalent to a distance of 4 km times 111 in binary, or 28 km. If we wanted to travel 20 km instead, we could connect the input and output of the 8-km connections together and connect the output of the 4-km path to the input of the 16-km path. This configuration would bypass the 8-km path so light would only travel through the 4-km path, then the 16-km path. This is equivalent to 4 km times 101 in binary, or 20 km. The 4-km fiber coils used Corning's LEAF fiber to mitigate dispersion, as described in the section on optical fiber. The coils were manufactured to have an outer diameter of 4.5 in., an inner diameter of 2.5 in., and height of 2 in. The fibers were potted to ensure that the fibers were not loose.
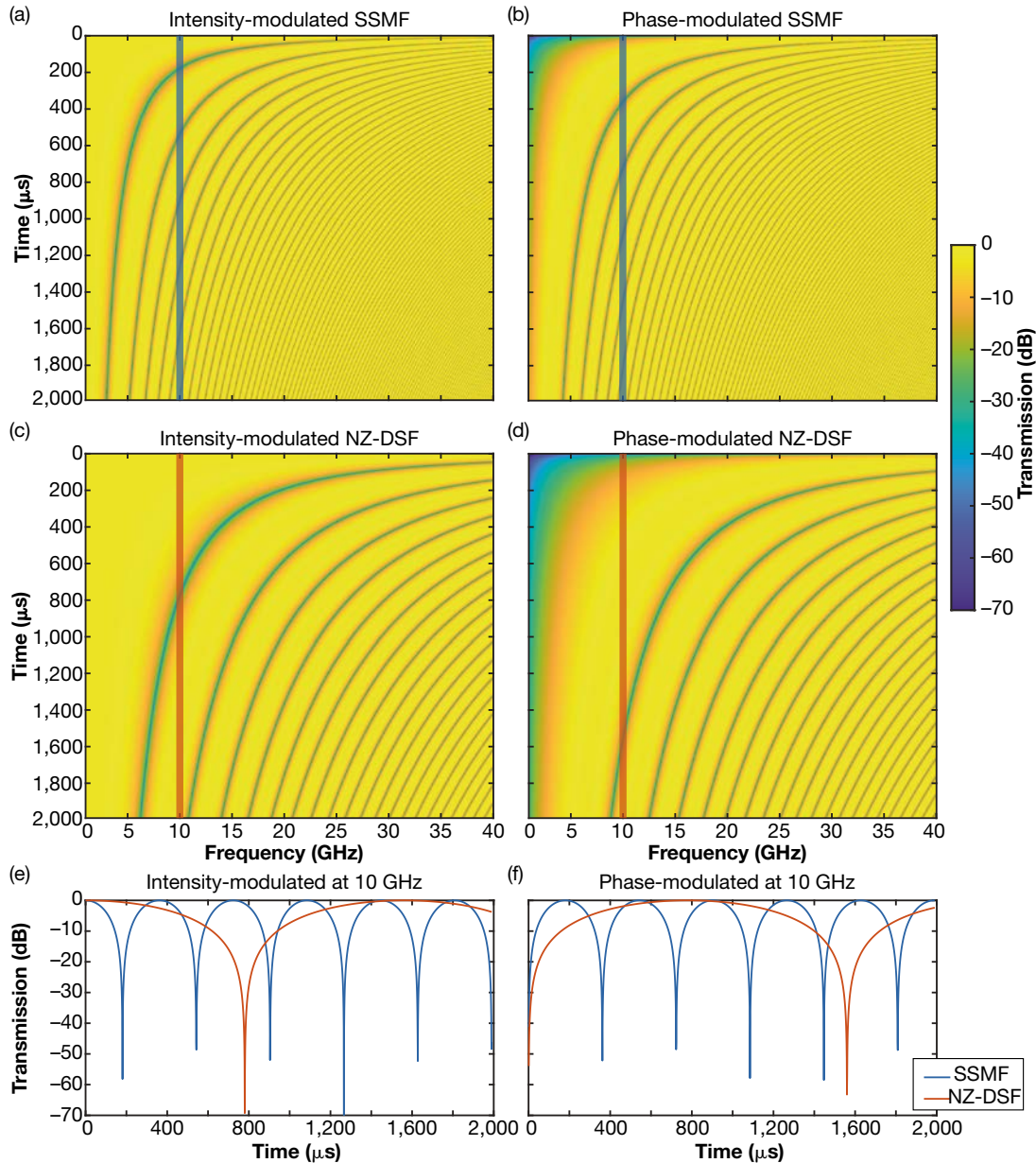

Figure 4. Simulated transmission as a function of the time (which corresponds to fiber length) and RF-modulated frequency. The plots on the left (a, c, and e) show an intensity-modulated signal, and the plots on the right (b, d, and f) show a phase-modulated signal. Because of chromatic dispersion, there are nulls in the RF response. Plots a and b show the response for SSMF. Plots c and d show the response for NZ-DSF. Plots e and f compare the transmission of SSMF (blue) and NZ-DSF (orange) fiber types at 10 GHz as a function of time. SSMF has more chromatic dispersion than the NZ-DSF fiber.
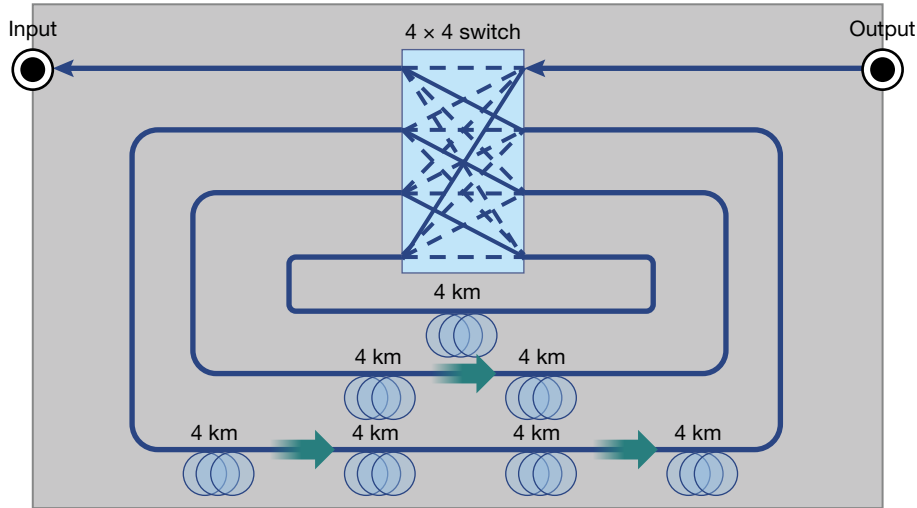
Figure 5. Switched architecture. The 4 × 4 matrix switch and fiber lengths allow for seven storage times from 20 to 140 µs in 20-µs increments.

Optical isolators are interspersed between longer fiber lengths to minimize back-reflection due to stimulated Brillouin scattering (SBS). Nonlinearities in the optical fiber can cause a large fraction of the input light to propagate in the backward direction and be amplified. While RCLs used for telecom data transport are not usually concerned with SBS, we are transporting relatively narrow band signals, and at our storage length, the input power would surpass the SBS threshold power limit.[12] Optical isolators are devices that only allow the transmission of light in one direction. Therefore, by placing isolators in the appropriate positions, we can attenuate the backward-propagating light to suppress the SBS reflections. We did not want to include more isolators than would be required to reduce the SBS threshold to an acceptable level since isolators add additional loss to the system. Therefore, we placed isolators in positions such that light does not travel more than ~8 km without isolation for all switch configurations.

This switched architecture helps reduce the number of recirculation events required for a desired transmission length. Eight loops are required for the 28-km fiber option instead of 50 for the 4-km option to store the signal for 1 ms. Since each recirculation amplifies the signals' noise floor, this switched architecture helps improve the RCL's signal-to-noise ratio. Having fewer circulations also reduces the amount of gain flatness required.

Gate Block

After the RF signal of interest is encoded onto a wavelength (or multiple wavelengths), optical signal is injected into the RCL for transport. Proper timing between the light injection into the loop and the light recirculating in the loop is essential: we need to open or close a crossbar optical switch (gate block) quickly enough so that light can either enter the loop or recirculate within the loop. The fiber length options were 4, 8, 12, 16, 20, 24, and 28 km, which correspond to storage times of approximately 20, 40, 60, 80, 100, 120, and 140 µs for each recirculation, respectively. Therefore, the timing for the switching was dependent on the user's desired storage time.

RCLs require optical switching to turn the transmitter on and fill the loop and turn it off to allow the data to circulate. We refer to the state when the light enters the loop as the load state and the state when the light is recirculating as the loop state. Historically, this switching has been done using two acousto-optic modulators (AOM) and a coupler.

The AOMs provide high extinction ratios (60—70 dB), low insertion losses (3 dB), low polarization dependence (<0.1 dB), and fast switching speeds (~200 ns).[13] Having a high extinction ratio is important for limiting the unwanted power that can leak into the loop when the RCL is in the loop state. The interferometric modulation adds noise to each circulation and thus reduces system performance. Although the AOM architecture meets our system switching requirements, because of our size constraints, we decided to implement a gate block that consists of three high-speed solid-state optical switches instead. We use 1 × 2 switches such that in one state, the signal from the encoder is connected to gate block output, and in the other state, the previously circulated signal is connected to gate block output. We needed switches with a sufficiently fast response time to load the light. Many vendors supply optical switches with low PDL/PMD and low insertion loss, but most are too slow for our system. We selected Agiltron 1 × 2 NanoSpeed switches to perform this function since the specification for the maximum response time was 300 ns, which is much shorter than the shortest storage time, 20 µm. For an individual switch, the typical specifications are 0.6 dB insertion loss, 0.15 dB PDL, and 0.1 ps PMD, which meets our requirements.[14] However, for an individual switch, we measured an extinction ratio of ~30 dB (Figure 6). This amount (30 dB) of crosstalk is equivalent to ~3% interferometric modulation. This level of interference is too high for our RCL, but this can be mitigated by cascading two switches in series. As shown in Figure 6, this reduces the extinction ratio to ~60 dB. At 60 dB extinction, the interferometric modulation is ~0.1% (<0.01 dB), which is well within acceptable levels.
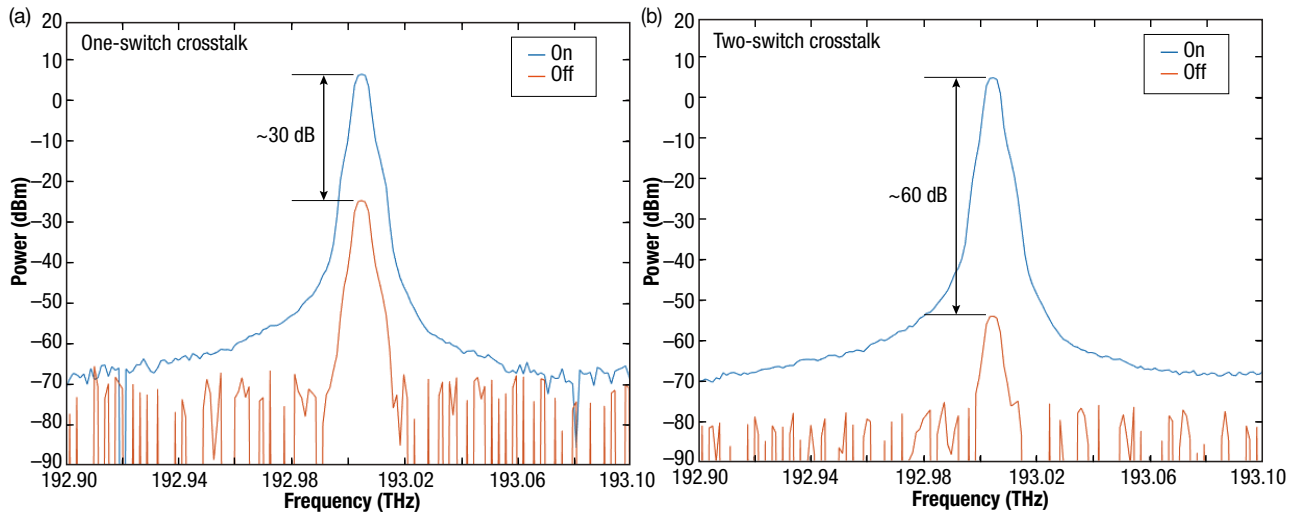
Figure 6. Measured switch crosstalk. For a single switch (a), the crosstalk is ~30 dB, which is too much for the RCL. For two switches connected together (b), the crosstalk is ~60 dB.

The implemented switch configuration is shown in Figure 7. In the load state, the switches allow light from the encoder to go into the loop and prevent light in the loop from continuing to recirculate. In the loop state, the switches prevent light from the encoder from going into the loop and allow light in the loop to continue recirculating. Note that the optical signals must pass through two switch elements on each path, thereby achieving the required isolation between light from the input and light circulating in the loop. The timing of the switches was controlled to hold them in the load state for the amount of time required to fully load the signal into the RCL based on the chosen fiber length and to then hold the loop state for the required 1-ms storage duration.

Amplification

While optical fibers have lower loss compared with coaxial cables, they still have loss of ~0.2 dB/km. Since the RCL will operate for a total length of 200 km of fiber and there are additional insertion losses associated with the other components in it, an amplifier is required to compensate for the losses. Without amplification, the signal would not be sustained for the required storage duration.

In Figure 8, we show the output of a photodiode as a function of time with and without amplification. This was a preliminary RCL benchtop test using only 6 km of SSMF and an erbium-doped fiber amplifier (EDFA) for amplification, which is discussed in the following paragraphs. The isolators discussed in the section on switched delay architecture are not included. The blue indicates the on/off trigger for the gate block switches. At the low trigger level, the RCL is in the load state, and at the high level, it is in the loop state. The orange line indicates the output voltage of the photodetector. Without an EDFA (Figure 8a), the light is only able to transport for about 90 μs before fully dissipating, much less than our required storage duration of 1 ms. With the EDFA (Figure 8b), we are able to extend the transport duration and maintain the optical power for a
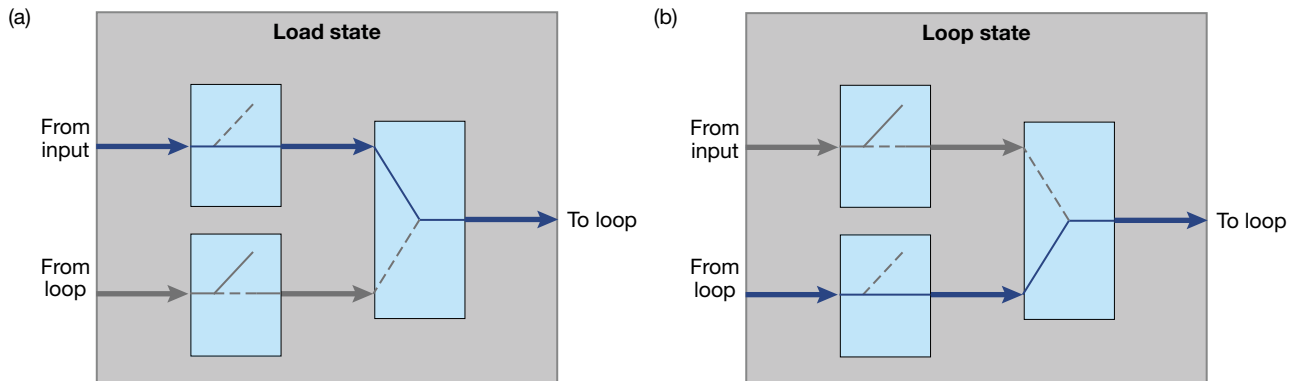

Figure 7. Gate block switch configuration. The blue shows the path that the light travels. In the load state (a), the input signal from the encoder goes into the loop. In the loop state (b), the input signal from the loop continues to recirculate in the loop.
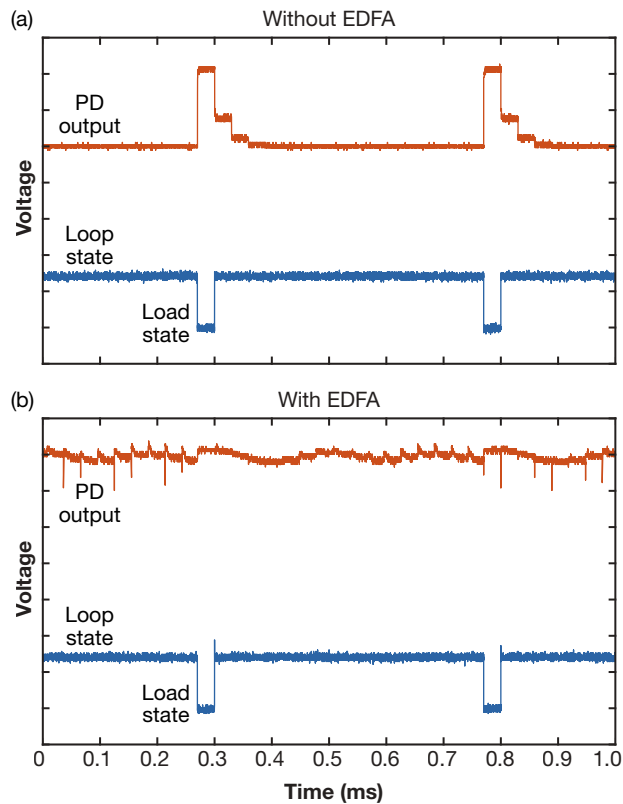
(a)

(b)

Figure 8. Output of photodiode (PD, orange) as a function of time with (a) and without (b) amplification. The blue line indicates whether the RCL is in the loop or load state. Without amplification, the power is lost after three loops. With amplification, the power is measurable for the entire storage duration.

longer period of time. Since isolators were not used in this RCL, the SBS threshold is surpassed, which limits the gain stability at the output and causes the non-flat photodiode output shown in the figure. To transport for the entire 1 ms with a constant gain for each circulation, isolation is required.

The most prevalent optical amplifier in the C-band is the EDFA. This amplifier operates via a pump light source at 980 nm, which excites erbium ions embedded in an erbium-doped fiber. From this excited state, the erbium ions can amplify light in the C-band via stimulated emission back to the ground state. This process converts pump light power to amplification efficiently (>50%) and amplifies a very wide wavelength band (>80 nm) with relatively flat gain. For this reason, the EDFA is the predominant optical fiber amplifier used in optical communication.

EDFAs have a non-flat gain spectrum across the C-band, meaning some wavelengths will be amplified more than others.[15] For the single-wavelength operation, the amplified spontaneous emission (ASE) peaks could be filtered out with the optical filter so that they do not compete with the laser power (see the Programmable Optical Filter section).

To enable transport of a WDM signal, we opted to use a gain-flattened EDFA. A gain-flattened EDFA includes a specially designed filter to cancel the variations in the gain spectrum at a specific combination of input and output optical signal powers. The drawback of using a gain-flattened EDFA is lower amplification. However, the lower amplification was sufficient for our fiber lengths. We selected Nuphoton's gain-flattened DWDM EDFA for our application because its low noise figure (5 dB) and gain (20 dB) matched our system requirements (maximum loss of ~18 dB loss per recirculation). Additionally, this low-gain EDFA model ensures that the output power (17 dBm) is less than the SBS threshold mentioned, as discussed in the Switched Delay Architecture section.

Programmable Optical Filter

The II-VI WaveShaper optical filter offers extremely fine control of filter parameters. The WaveShaper is a liquid-crystal-on-silicon optical processor consisting of a matrix of reflective liquid crystal elements. With an applied voltage, individual matrix elements can shift the phase of corresponding spectral components. This allows for attenuation and phase control of a given wavelength without interfering with other wavelengths. In addition to this versatility, we chose a programmable filter so that the RCL design works in both single-channel and WDM operation.

We included the II-VI WaveShaper in the RCL design to serve two purposes: (1) precise bandpass filtering of each optical channel and (2) dispersion compensation. Foremost, bandpass filtering of each optical channel (for single- or multi-channel operation) blocks out ASE noise that would otherwise be amplified with each recirculation. Each bandpass filter is centered on a transmission channel and is 100 GHz wide, so signals up to 50 GHz are transmitted while undesired signals are filtered out. Moreover, we can individually control the attenuation of each channel to counteract any undesired wavelength-dependent loss from the elements within the loop (most notably the amplifier). As an added bonus, the WaveShaper supports wavelength-dependent dispersion compensation—up to ±50 ps/nm compensation for 50-GHz channels—meaning that we can use the WaveShaper to eliminate all chromatic dispersion in NZ-DSF fiber lengths up to 28 km. We demonstrate enhanced performance by using dispersion compensation, discussed in the section on characterization.

Polarization Control

Each optical element within the RCL has a non-zero amount of PMD and PDL, which adversely affects the RCL's performance. Generally, polarization effects are small in long-distance transport. However, since a recirculating signal sees the same optical components

multiple times, any polarization effects multiply with each recirculation.

PDL is the insertion loss variation when an optical component is exposed to all possible polarization states. As a signal propagates through the RCL, optical components change the state of polarization, resulting in an overall PDL that changes from run to run. This differs from a long-haul transmission system, where PDL is consistent for each long-haul transmission.

PMD is caused by imperfections in the fiber manufacturing process, resulting in random birefringence along the length of the optical fiber. As a result, the light polarized in one axis of polarization travels at a different speed than the light polarized in the orthogonal axis, causing pulse broadening. To first order, PMD can be represented by the differential group delay (DGD), which is the difference in propagation time between the two orthogonal polarization modes. A long-haul transmission fiber displays birefringence randomly along the fiber length. As a result, the DGD displays a Maxwellian probability density function, and the mean DGD increases with the square root of fiber length. However, because of the periodic structure of an RCL, it does not display the same statistical properties of a randomly birefringent long-haul fiber. Instead, in a conventional RCL, the mean DGD grows linearly with fiber length, and the probability density function approaches a uniform distribution. This means that a large DGD is very likely to occur, resulting in worse PMD performance than in a standard long-haul system.

Luckily for us, it has been shown that an RCL can reproduce the Maxwellian DGD statistics if the state of polarization of light is scrambled synchronously with each circulation of light within the loop.[2] This can be performed using an optical component known as a polarization scrambler. Additionally, a polarization scrambler results in consistent run-to-run PDL. As such, a loop-synchronous polarization scrambler is necessary in the development of modern RCLs.

Mechanical, Power, and Control

The final RCL system is shown in Figure 9, where all components are placed in a 3U × 18-in.-depth chassis. The seven fiber spools are placed on the bottom half,
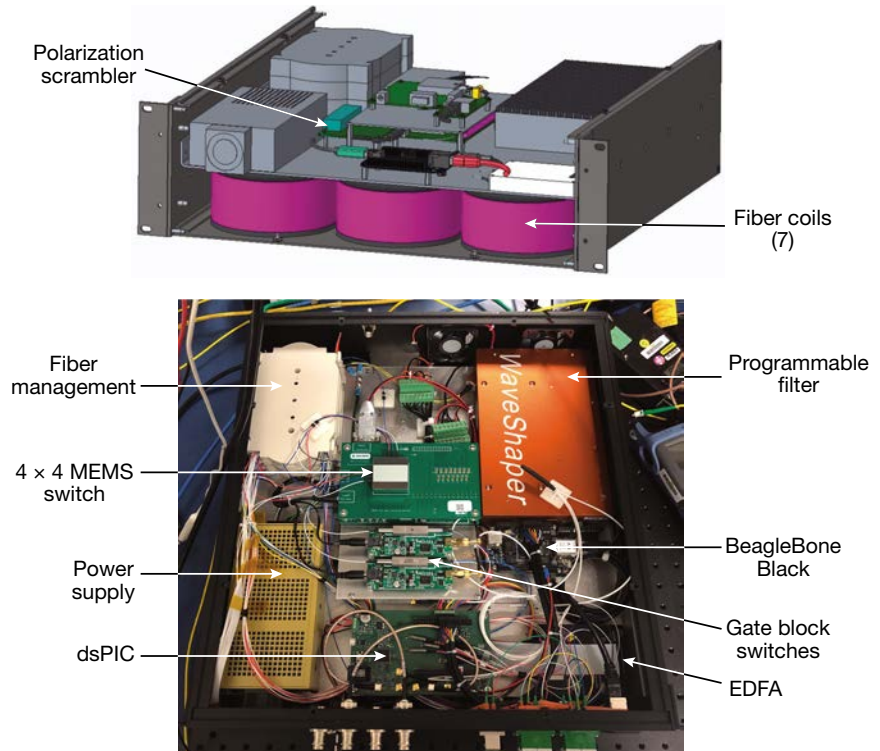

Figure 9. CAD model and top view of final system. Components were fit into a 3U × 18-in.-depth chassis.

while the rest of the components are placed above on a shelf. All fiber splicing is contained within three splice trays shown in the upper left corner.

For communication, we used a BeagleBone Black as a single board processor to communicate with all Ethernet and universal asynchronous receiver-transmitter (UART) devices. The BeagleBone Black also communicated via I2C to a dsPIC microcontroller, which performed the high-speed input/output required for loop-synchronous polarization scrambling and gate block triggering. The end user communicates to the system via a Telnet interface to the BeagleBone Black. Moreover, the BeagleBone Black includes a script to automatically balance the power within the loop by adjusting variable optical attenuators based on the power read from tap monitors placed throughout the loop. Therefore, the only settings the user needs to set via the Telnet interface are transmission length (4–28 km) and single-channel or WDM mode.

CHARACTERIZATION

In this section, we discuss the characterization of the RCL to understand how the design decisions improved the performance. To characterize the system, we placed the RCL in a photonic link as shown in Figure 10. We used an RF function generator to modulate an optical continuous-wave source using an E/O modulator.
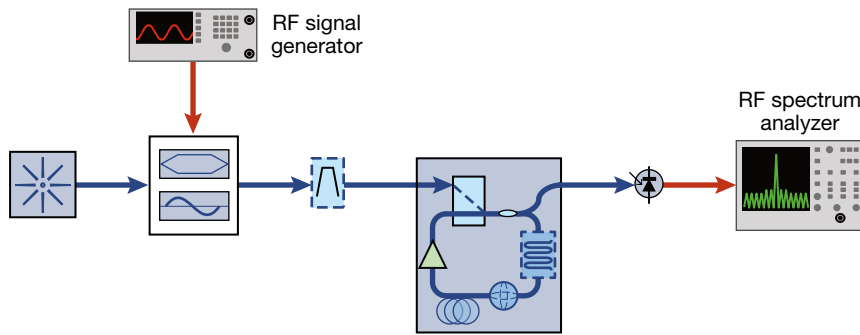
Figure 10. Block diagram of RCL system characterization. A continuous-wave source is modulated by an RF signal supplied by an RF function generator. The modulated signal is sent to the RCL. The power at the output of the RCL is measured at each given frequency as a function of time using a photodiode and spectrum analyzer.
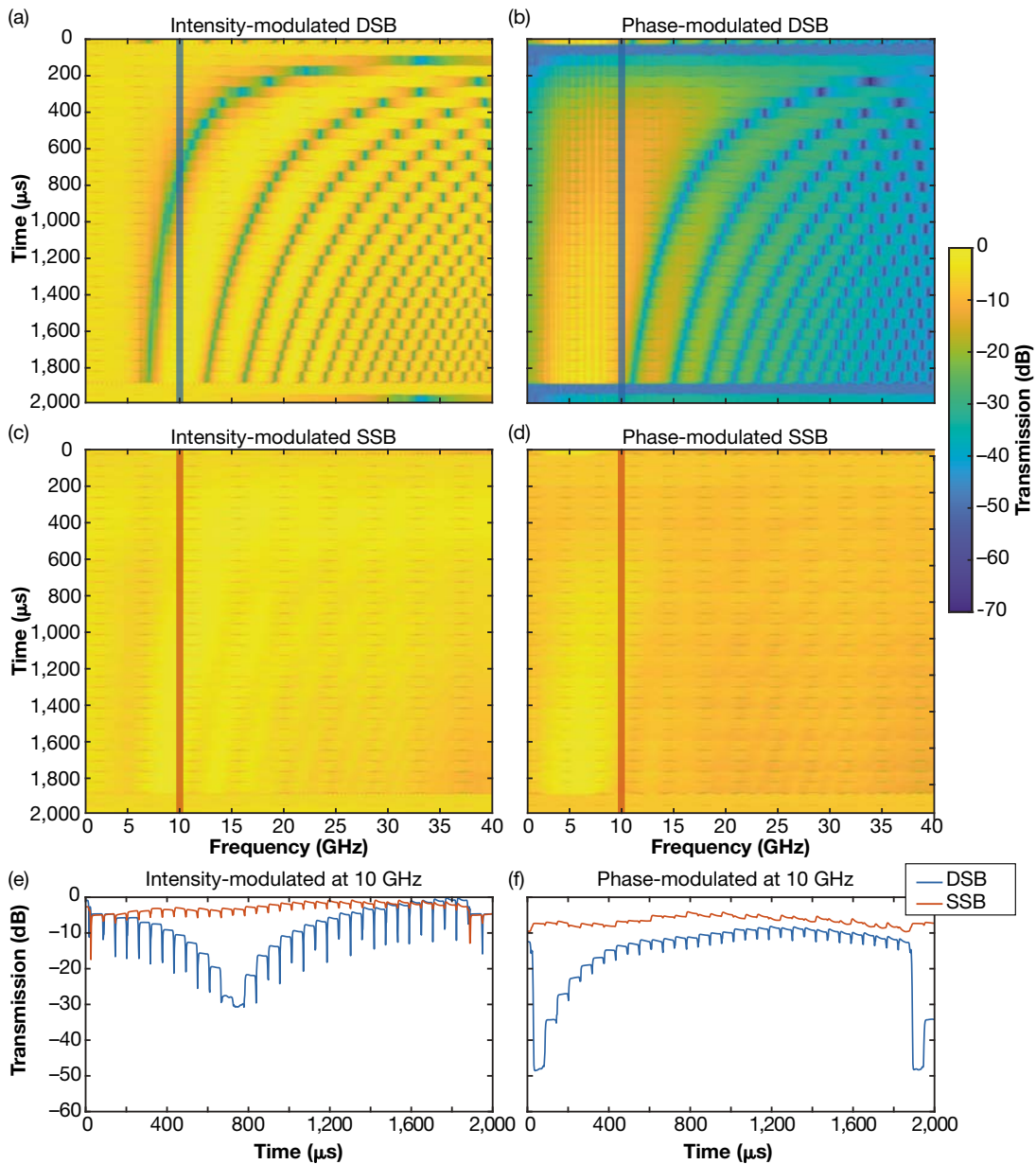

Figure 11. RF transmission at the output of the RCL. Measurements are shown as a function of time and frequency for intensity-modulated DSB (a), phase-modulated DSB (b), intensity-modulated SSB (c), and phase-modulated SSB (d). Plots e and f show frequency cuts at 10 GHz. With an SSB signal, the null signals are not as strong because the chromatic dispersion is reduced.

We characterized the system for both intensity- and phase-modulated signals. For comparison purposes, we either included or omitted the filter used to convert the DSB signal to SSB. Then the modulated light was sent to the RCL and the power was measured at the output. We swept the generated RF frequency from 1 to 40 GHz in 0.1-GHz increments at each given frequency as a function of time using a spectrum analyzer at the output of the photodiode.

Figure 11 demonstrates the effectiveness of using an SSB signal versus a DSB signal to reduce the effects of dispersive fading for both intensity- and phase-modulated signals. The plots on the left show an intensity-modulated signal, and those on the right show a phase-modulated signal. In this example, we used a 12-km fiber length of NZ-DSF, which corresponds to 60-µs storage times. Plots a and b show the transmission for intensity- and phase-modulated DSB signals, respectively. Notice that plots a and b in Figure 11 correspond to and agree with the modeled plots c and d in Figure 4. As mentioned previously, this behavior due to chromatic dispersion is not ideal for long distances and high frequencies. To

increase the signal's flatness, we filtered out one of the sidebands and measured the SSB signal's response. As shown in plots c and d of Figure 11, switching to an SSB signal produced a significantly flatter response across all frequencies for the entire storage duration for both the intensity- and phase-modulated signals. Looking at the 10-GHz cuts (plots e and f), we can see the response of each circulated copy in the DSB and SSB cases. Looking at the NZ-DSF results in Figure 4 (e and f) and the DSB results in Figure 11 (e and f), the RF power is not flat for each copy at 10 GHz. By instead using an SSB signal, we were able to generate a strong response for each copy for both modulation types. We also note that the raw data exhibit a roll-off at higher frequencies due to the bandwidth limitations of the photodetector. In this example, we normalize the power at each frequency to the load state response in postprocessing to ignore the effects from the photodetector roll-off.

Rather than using postprocessing to adjust the system power, we have the programmable optical filter available to adjust for the photodiode roll-off and the frequency-dependent behavior of the components. In Figure 12, we
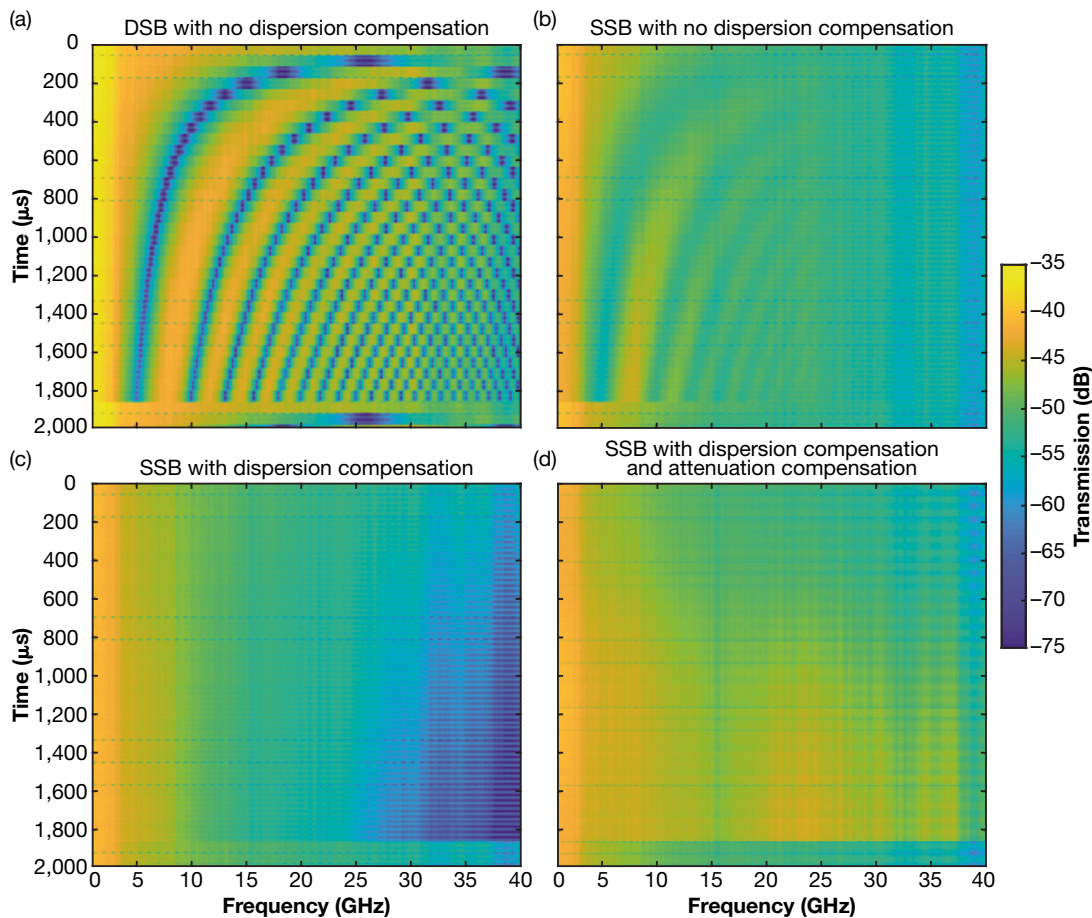

Figure 12. RF transmission at the output of the RCL. Measurements are shown as a function of time and frequency for intensity-modulated signals for a DSB signal without dispersion compensation (a), an SSB signal without dispersion compensation (b), an SSB signal with dispersion compensation (c), and an SSB signal with dispersion and attenuation compensation (d). Dispersion and attenuation compensation results in the smallest amount of dispersive fading and provides power normalization.

D. M. Moody and J. A. Shackford

demonstrate the effectiveness of using the programmable optical filter for both additional dispersion compensation and attenuation compensation. We show the intensity-modulated response using 12 km of NZ-DSF. Plots a and b in Figure 12 show a DSB and SSB transmission without dispersion compensation, analogous to the result for plots a and c in Figure 11. In Figure 12, we do not apply postprocessing attenuation normalization; therefore, the RF power is lower at higher frequencies. Also, since the range of powers plotted in Figure 12 is smaller, it illustrates more clearly the residual dispersion nulls that still occur even when switching to an SSB signal. To address the residual dispersion compensation, the programmable optical filter dispersion compensation is shown in Figure 12c. Comparing plot b and c shows that the dispersion nulls are eliminated from the response. However, there is still an attenuation roll-off in plot c. In plot d, we show a SSB signal with both dispersion and attenuation compensation. Applying both dispersion and attenuation compensation results in the smallest amount of dispersive fading and provides power normalization for the system.

SUMMARY

Microwave photonics enables RF signals to be processed in the optical domain, which offers several advantages over traditional signal processing systems. Namely, optical fiber enables low-loss, long-distance transmission, which is particularly useful for communication. In this article, we walked through the design of an RCL that mimics the behavior of a long-haul transmission system with the benefit of fitting in a small form factor.

We designed the RCL to generate multiple copies of an input RF signal. Our system was designed to receive either an intensity- or a phase-modulated signal in either single- or multiple-wavelength operation. The RCL design consisted of a gate block, a programmable optical filter, polarization control, a switched delay architecture, and an amplifier. The input signal enters the RCL through the gate block and passes through the optical filter and polarization scrambler. The light travels through a length of fiber that is selected from 4 km to 28 km at the switched delay architecture. Then, the light is amplified to match the input power. The light circulates multiple times for a total storage duration of 1 ms. For each component in the system, design decisions were implemented to mitigate photonic effects, including dispersion, loss, crosstalk, polarization, and SBS. The entire module is controlled through a Telnet interface and was included in a 3U chassis with the rest of the prototype. We showed that we could generate repeated copies of a single wavelength and WDM signals with high fidelity.

REFERENCES

[1]A. J. Seeds, C. H. Lee, and M. Naganuma, "Guest editorial: Microwave photonics," *J. Lightw. Technol.*, vol. 21, no. 12, pp. 2959–2961, 2003, https://doi.org/10.1109/JLT.2003.822323.

[2]J. Capmany, B. Ortega, and D. Pastor, "A tutorial on microwave photonic filters," *J. Lightw. Technol.*, vol. 24, no. 1, pp. 201–229, 2006, https://opg.optica.org/jlt/abstract.cfm?uri=jlt-24-1-201.

[3]A. V. Oppenheim, A. S. Willsky, and I. T. Young, *Signals and Systems*, 1st ed., Prentice Hall, 1983.

[4]C. Yeh, *Handbook of Fiber Optics Theory and Applications*, Academic Press, 1990.

[5]V. J. Urick Jr., J. D. McKinney, K. J. Williams, *Fundamentals of Microwave Photonics*, Wiley, 2015.

[6]*Characteristics of a single-mode optical fibre and cable*, ITU-T Standard G.652, ITU Telecommunication Standardization Sector (ITU-T), 2017, https://www.itu.int/rec/T-REC-G.652/en.

[7]*Characteristics of a dispersion-shifted single-mode optical fibre and cable*, ITU-T Standard G.653, ITU Telecommunication Standardization Sector (ITU-T), 2010, https://www.itu.int/rec/T-REC-G.653/en.

[8]K. Inoue, "Four-wave mixing in an optical fiber in the zero-dispersion wavelength region," *J. Lightw. Technol.*, vol. 10, no. 11, pp. 1553–1561, 1992, https://doi.org/10.1109/50.184893.

[9]*Characteristics of a non-zero dispersion-shifted single-mode optical fibre and cable*, ITU-T Standard G.655, ITU Telecommunication Standardization Sector (ITU-T), 2009, https://www.itu.int/rec/T-REC-G.655/en.

[10]"Corning® SMF-28® ULL Optical Fibers," Corning, https://www.corning.com/optical-communications/worldwide/en/home/products/fiber/optical-fiber-products/smf-28-ull.html (accessed May 6, 2022).

[11]"Corning® LEAF® Optical Fiber," Corning, www.corning.com (accessed May 6, 2022).

[12]G. Agrawal, *Nonlinear Fiber Optics*, Academic Press, 2013.

[13]N. S. Bergano and C. R. Davidson, "Circulating loop transmission experiments for the study of long-haul transmission systems using erbium-doped fiber amplifiers," *J. Lightw. Technol.*, vol. 13, no. 5, pp. 879-888, 1995, https://doi.org/10.1109/50.387805.

[14]Agiltron, "NanoSpeed™ 1 × 2 series fiber optical switch," revised April 25, 2022, https://cdn-agl.agiltron.com/dlc/specs/NS_1x2_switch_All.pdf.

[15]P. C. Becker, N. Anders Olsson, and J. Simpson, *Erbium-Doped Fiber Amplifiers: Fundamentals and Technology*, 1st ed., Academic Press, 1999.

Diamond M. Moody, Air and Missile Defense Sector, Johns Hopkins University Applied Physics Laboratory, Laurel, MD

Diamond M. Moody is a member of the Optics and Photonics group in APL's Air and Missile Defense Sector. She received her BS in applied physics with a minor in engineering studies from Carnegie Mellon University and her MS in applied physics from Johns Hopkins University. The Optics and Photonics Group was her first rotation in APL's Discovery Program. She also rotated through the Operational and Threat Assessment Group in the Force Projection Sector, the Multifunctional Materials and Nanostructures Group in the Research and Exploratory Development Department, and the Space Environmental Effects Engineering Group in the Space Exploration Sector. On this project, she focused on building and testing a lab prototype for single-wavelength operation of the recirculating loop. Her email address is diamond.moody@jhuapl.edu.

James A. Shackford, Research and Exploratory Development Department, Johns Hopkins University Applied Physics Laboratory, Laurel, MD

James A. Shackford is a member of the Experimental and Computational Physics group in APL's Research and Exploratory Development Department. He received his BS in physics, electrical and computer engineering, and computer science from Duke University. He is currently pursuing his MS in electrical and computer engineering with a photonics concentration from Johns Hopkins University. The Optics and Photonics Group was his second rotation in the Discovery Program. He also rotated through the Experimental and Computational Physics Group, the Space and Missile Defense Applications Group in the Space Exploration Sector, and the Electro-Optical and Infrared Systems Group in the Air and Missile Defense Sector. On this project, he further developed the prototype to function for multiple wavelength operation and assembled the final system. His email address is james.shackford@jhuapl.edu.